Received June 2002
Revised January 2002
Accepted April 2003

The propagation of temperature and concentration fields around a deformed gas bubble rising in a quiescent hot or bi-solution liquid

W.Z. Li, Y.Y. Yan and J.B. Hull
School of Engineering, The Nottingham Trent University, UK

Keywords *Numerical analysis, Simulation, Heat transfer, Liquids*

Abstract *This paper is concerned with a numerical study on evolution of a deformed bubble and propagation of the fields around the bubble. The model uses a numerical procedure with the direct-predictor method and the alternating dependent variables (ADV) skill developed by Li and Yan. The aim of this paper is to study the characteristics of interfacial transport for a deformed inviscid bubble rising in a quiescent hot or bi-solution liquid. The effects of the bubble deformation on temperature and concentration fields are calculated and simulated. The results demonstrate that the current numerical procedure is effective for solving such unsteady deformation problems of bubble accompanied with heat and mass transfer.*

Nomenclature

A_b = constant coefficient
C = concentration
C_D = drag coefficient
d_e = bubble equivalent diameter (m)
Eö = Eötvös number $\left(= \Delta\rho g d_e^2/\sigma\right)$
F_x = drag force in the x-direction
J = Jacobian transformation number
Mo = Morton number $(= g\mu^4/\rho\sigma^3)$
p = pressure (Pa)
r = coordinate (m)
Re = Reynolds number $(= \rho V_T d_e/\mu)$
S = source term in general governing equation
t = dimensionless time $(= t' U_T/d_e)$
t' = realistic time (s)
T = temperature (K)
u = Cartesian velocity component in the x-direction (m s^{-1})
$\bar{u}_T$ = dimensionless terminal velocity $(= u_T/U_T)$
v = Cartesian velocity component in the r-direction (m s^{-1})
U = contravariant velocity component
V = contravariant velocity component and bubble volume (m^3)
U_T = bubble terminal rising velocity (m s^{-1})
We = Weber number $(= \rho U_T U_T d_e/\sigma)$
x = coordinate (m)
α = covariant metric tensor

The authors wish to acknowledge the support given by the Faculty Fund of the Nottingham Trent University and the EPSRC grant GR/M90207 for this work. After being awarded his PhD, W.Z. Li is now working in the Department of Power Engineering, Dalian University of Technology, China.

International Journal of Numerical Methods for Heat & Fluid Flow
Vol. 13 No. 8, 2003
pp. 940-963

0961-5539
DOI 10.1108/09615530310501911

β = covariant metric tensor or constant coefficient
δ = difference operator
ϕ = general dependent variable
γ = covariant metric tensor
η = coordinate in computational space
μ = dynamic viscosity ($kg\,m^{-1}\,s^{-1}$)
ρ = density ($kg\,m^{-3}$)
σ = surface tension coefficient ($N\,m^{-1}$)
τ = shear stress
ξ = coordinate in computational space
Δ = gradient operator
Γ = diffusion coefficient
$\mathscr{R}$ = ratio of bubble volume at the present step to the last

Subscripts

b = values at the interface
$b-1$ = values on the point one grid away from the interface
e = equivalent
∞ = value at the reference point
o = values of the gas inside bubble
τ = tangential direction

Superscripts

old = values at the last iteration step
new = values at the present iteration step
n = values at the last iteration step
p = values at the predictor phase
$n+1$ = values at the present iteration step

Introduction

A bubble's deformation is an important behaviour when the bubble rises freely in a quiescent liquid. This is because the deformation has significant effects not only on the flow around the bubble, but also on other transport characteristics. For example, when a deformable bubble rises in a quiescent hot or bi-solution liquid, heat and mass will transfer across the interface. The rate of transportation is dependent on the temperature and concentration gradients formed by both diffusion and convection, which are induced by the flow field. Therefore, the deformation of a rising gas bubble is a result of interactions of interfacial stresses, including the surface tension forces, hydrostatic and dynamic pressures, and viscous forces. The shape of the bubble is dependent on the characteristics of the flow around it; meanwhile, the characteristics of flow actually results from the bubble shape. In fact, these interactions constitute a complicated and intrinsic moving boundary problem in thermo-fluid dynamics; on this, the movement of a gas-liquid interface must be calculated as a part of the solution and the grid used has to move with the interface. In an earlier work, the authors have developed a direct-predictor method (Li and Yan, 2002a) with an alternating dependent variables (ADV) skill (Li and Yan, 2002b) to simulate the problem of a steadily deforming bubble. Complete solutions including the steady terminal bubble shapes have been obtained. However, for the problem of time-dependent bubble deformation, when the grid points move to new positions, the accumulation of the artificial mass source does not occur during the solution for the flow field. Because there is no time derivation term in all the governing equations, the variable values at the last iteration step do not influence those at the current step. In addition, if the flow is considered as unsteady, the volume of each cell in the computational domain changes with grid movement; this will result in the accumulation of the artificial mass source with time marching. As pointed out by Dermirdzic and Peric (1988, 1990), mass conservation must be obtained by

enforcing the so-called space conservation law (SCL), which will be discussed later.

This paper is concerned with the development of a method to solve the unsteady free-boundary problems in thermo-fluid dynamics. Although the solution approach for a steady free-boundary problem has been developed by Li and Yan (2002a,b), an unsteady technique is essential to understand certain types of fluid mechanics problem, such as the effect of unsteady deformation of a bubble on temperature and concentration fields, and on the evolution of bubble shape; it may also play an important role in understanding the limitations encountered by steady algorithms in obtaining solutions for some parameter values. For example, in the unresolved problem of a rising bubble in a quiescent liquid, a transient approach may either lead to a stable steady solution on a new branch or reveal the lack of steady solutions. In this paper, the general features of a new numerical algorithm for transient, free-boundary problems will be introduced, which will then be applied to the specific problem of unsteady deformation of a bubble in a viscous incompressible Newtonian fluid that undergoes an external flow.

The existing literature on numerical methods for unsteady free-boundary problems is quite limited. However, two classes of solution methods can be identified. One is the so-called boundary-integral technique, which has been applied to a wide range of problems with an initial shape. Although it is extremely powerful when applied, the method is currently restricted to the limiting cases of either zero Reynolds number or for an inviscid irrotational flow; this indeed reduces its general usefulness. The other, a more general class of solution methods, is a full numerical technique that is suitable when the governing equations are non-linear. In this class, three distinct methods are summarised.

The first is the marker and cell (MAC) method, which employs the Eulerian mesh of computational cells and finite difference expressions to approximate the governing equations, and in addition, a set of marker particles that moves with the fluid to track the position of free surface is used. This method has been successfully applied to very largely deformed free surfaces, but usually with surface tension neglected. However, the intrinsic difficulty is that the surface position does not generally coincide with the given mesh points. Thus, a special kind of interpolation technique must be used to apply the boundary conditions.

The second method is a finite-element method, which has been used to obtain most of the existing solutions of unsteady free-surface problems. In this, the strategy for deforming the elements is the most critical factor in successful applications. Usually, for either a Lagrangian approach or a flow-independent scheme, the element's deformation is only determined by the boundary shape at each instant. Therefore, the motion of the element nodes is independent of the velocity field of fluid.

Moreover, on the basis of Ryskin and Leal's (1984a-c) steady method, Kang and Leal (1987, 1989) proposed a third method suitable for unsteady free-boundary flow problems. In their method, a finite difference method was used to discrete the vorticity-stream function of Navier-Stokes equations. The new interface points were modified by using the imbalance normal stress and combining it with an orthogonal mapping technique. This method was used to simulate gas bubble deformation in an uni-axial straining flow and biaxial straining flow (Kang and Leal, 1989). Takagi *et al.* (1997) have employed the orthogonal boundary fitted coordinate (BFC) to solve the full Navier-Stokes equations. However, in these researches, the only focus was on the fluid dynamics, the heat and mass transfer accompanying bubble deformation have not been considered in the open literature.

In this paper, an unsteady bubble deformation in external flow is calculated by using the SIMPLE method; a non-orthogonal BFC is used to match the interface of a deformed bubble; and the ADV skill (Li and Yan, 2002b) is employed to treat the slip-boundary conditions to circumvent the numerical instability resulted from the zero and infinite slope of the bubble profile. In addition, propagation of the temperature and concentration fields is simulated in order to understand the evolution of the bubble deformation.

Problem formulation

Assumptions

On the basis of Plesset and Zwick's (1954) and Ryskin and Leal's (1984a-c) studies, the following assumptions have been made:

(1) the gas-liquid interface is completely free of surfactant;

(2) both the boundary geometry and flow fields are axisymmetric;

(3) the bulk liquid is an incompressible Newtonian fluid, its density and viscosity being sufficiently large when compared with those of a gas; and

(4) the dynamic pressure and stresses at the interface are negligible on the gas side compared with those on the liquid side.

Coordinate system and grid generation

In this paper, non-orthogonal BFC of (ξ, η, θ) are employed, where θ is the azimuthal angle, measured about the axis of symmetry. With the assumption of axisymmetry, these non-orthogonal coordinates can be connected with common cylindrical coordinates (x, r, θ) as shown in Figure 1. The corresponding grid is generated using the numerical grid generation technique developed by Thompson *et al.* (1974). In the present study, the technique for generating a transformed coordinate system as solutions of an elliptic differential system in the physical space is applied to a single-connected region

with arbitrarily shaped bubbles. The point (x, r) in the physical space satisfies the following elliptic equations in the non-orthogonal BFC system (ξ, η)

$$\alpha x_{\xi\xi} - 2\beta x_{\xi\eta} + \gamma x_{\eta\eta} + J^2(Px_\xi + Qx_\eta) = 0, \tag{1}$$

$$\alpha r_{\xi\xi} - 2\beta r_{\xi\eta} + \gamma r_{\eta\eta} + J^2(Pr_\xi + Qr_\eta) = 0 \tag{2}$$

where α, β and γ are metric tensors defined as follows:

$$\alpha = x_\eta^2 + r_\eta^2, \tag{3}$$

$$\beta = x_\xi x_\eta + r_\xi r_\eta, \tag{4}$$

$$\gamma = x_\xi^2 + r_\xi^2, \tag{5}$$

where J is the transformation Jacobian number given by

$$J = x_\xi r_\eta - x_\eta r_\xi. \tag{6}$$

The mathematical problem defined by equations (1)-(6) is subject to appropriate boundary conditions and constitutes the boundary value problem of numerical grid generation. In the present calculations, grid control functions P and Q in equations (1) and (2) are determined by the method described by Thomas and Middelcoff (1980). This method has advantages that the grid generated is normal to the physical boundary and the grid concentration in the computational domain is easy to control. With respect to the (ξ, η) system, the mapping is always defined in such a way that the solution domain is a unit square defined by $0 \leq \xi \leq 1$, and $0 \leq \eta \leq 1$.

The grid of non-orthogonal BFCs at the physical space is shown in Figure 2, where the curvilinear line for $\eta = 0$ fits the gas-liquid interface.

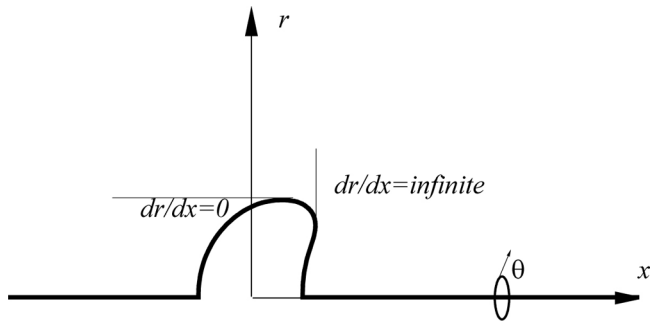

Figure 1.
Bubble shape and cylindrical coordinate system

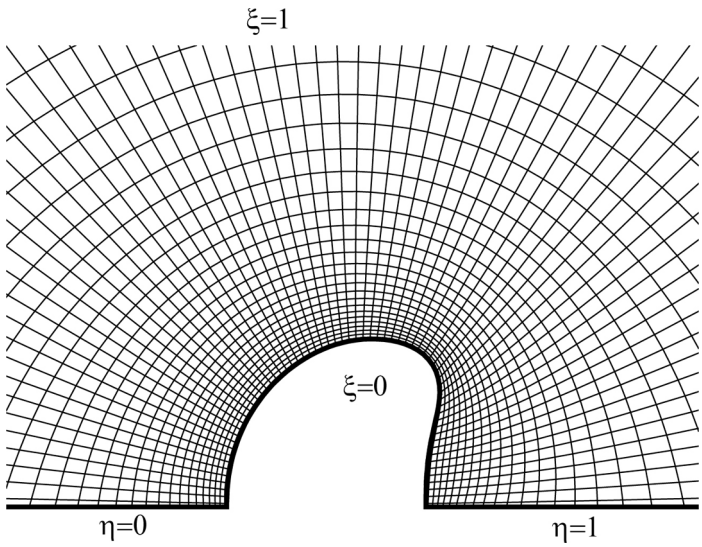

Figure 2.
Non-orthogonal BFC and grid generation

Governing equations and their discretisation

By earlier assumptions, determination of the flow with heat and mass transfer around a rising freely bubble needs the solution of the unsteady axisymmetric Navier-Stokes, energy and species continuity equations. Unlike most of the earlier works which addressed flow past a sphere and solved the Navier-Stokes equations by the vorticity and stream-function approach in orthogonal curvilinear BFCs, the formulation adopted in the present study is based on the primitive velocity-pressure variables in non-orthogonal BFCs. The equations developed are written in general non-orthogonal (as opposed to orthogonal) coordinates. These choices give much flexibility and allow the code to treat flow and heat transfer problems in an arbitrary computational domain with complicated geometry boundaries. In a non-orthogonal coordinate, there are several options for grid arrangement and the choice of dependent variables for momentum equations. The simplest of these is a straightforward extension of the formulation in Cartesian coordinate system (x, r). This involves staggering along the coordinate directions with one Cartesian velocity component stored at each face of the control-volume (Shyy *et al.*, 1996). In this paper, the Cartesian velocity components (u, v) are employed as dependent variables to predict flow and heat and mass transfer at the interface. In the investigation of time-dependent bubble deformation, the moving boundary must be solved as part of the solution for continuity and momentum equations. The velocities in the convection term in governing equations must be replaced by relative velocities U_r and V_r. The conservation equations for a general dependent variable ϕ in a non-orthogonal coordinate system (ξ, η) is then rewritten in the following general form:

$$\frac{\partial \rho J \phi}{\partial t} + \frac{\partial}{\partial \xi} r \left[\rho U_{\mathrm{r}} \phi - \frac{\Gamma}{J} \left(\alpha \frac{\partial \phi}{\partial \xi} - \beta \frac{\partial \phi}{\partial \eta} \right) \right] + \frac{\partial}{\partial \eta} r \left[\rho V_{\mathrm{r}} \phi - \frac{\Gamma}{J} \left(-\beta \frac{\partial \phi}{\partial \xi} + \gamma \frac{\partial \phi}{\partial \eta} \right) \right] = rJS(\xi, \eta) \tag{7}$$

where

$$U_{\mathrm{r}} = (u - u_g) \frac{\partial r}{\partial \eta} - (v - v_g) \frac{\partial x}{\partial \eta}, \tag{8}$$

$$V_{\mathrm{r}} = (v - v_g) \frac{\partial x}{\partial \xi} - (u - u_g) \frac{\partial r}{\partial \xi} \tag{9}$$

where U_{r} and V_{r} are the contravariant velocity components, $S(\xi, \eta)$ is the source term of ϕ in the (ξ, η) coordinates, Γ is diffusion coefficient, which represents mass coefficient in chemical species equations, dynamic viscosity coefficient in momentum equations, and thermal conductivity in energy equations, respectively. The general dependent variable ϕ equals 1, u, v, T and C, respectively.

The finite-volume method is applied in the discretisation of the governing equations. With a staggered grid arrangement, scalar quantities are located at the geometric centre of the control volume; velocity components are displaced in two coordinate directions, respectively, to lie at the midpoints of the control-volume faces.

Boundary conditions

According to Wittke and Chao (1967), the behaviour of a gas bubble rising at a variable velocity in a liquid of an infinite extent is equivalent to that of a bubble whose centre of mass is at rest while the unbounded liquid flows downward with a variable velocity, V_{T}, at a large distance away from it. For this situation, boundary conditions at the inlet of the solution domain are given as follows:

$$u = V_{\mathrm{T}}(t) \tag{10a}$$

$$v = 0 \quad \text{at any time} \tag{10b}$$

$$T = T_\infty, \quad \text{for heat transfer problem;} \tag{10c}$$

$$C = C_\infty, \quad \text{for mass transfer problem.} \tag{10d}$$

The boundary conditions at the outlet of the domain are given by zero normal velocity gradient and zero tangential velocity, and expressed as

$$\frac{\partial u}{\partial x} = 0, \tag{11a}$$

$$v = 0, \tag{11b}$$

$$\frac{\partial T}{\partial x} = 0, \tag{11c}$$

$$\frac{\partial C}{\partial x} = 0. \tag{11d}$$

Due to the assumption of axisymmetric flow, symmetric boundary conditions are given as:

$$\frac{\partial u}{\partial r} = 0, \tag{12a}$$

$$v = 0, \tag{12b}$$

$$\frac{\partial T}{\partial r} = 0, \tag{12c}$$

$$\frac{\partial C}{\partial r} = 0 \tag{12d}$$

The temperature and concentration boundary conditions are imposed for the interface as

$$u = 0, \tag{13a}$$

$$v = 0, \tag{13b}$$

$$T = T_b, \tag{13c}$$

$$C = C_b. \tag{13d}$$

As zero mass flux across the interface is assumed in the present study, the kinematic boundary condition becomes a zero relative normal velocity and is expressed as:

$$\frac{(v - v_g)x_\xi - (u - u_g)r_\xi}{\sqrt{\gamma}} = 0 \tag{14}$$

where subscript g stands for interfacial velocity; and the dynamic boundary conditions are written as:

$$\tau_\tau = \mu\left[x_\xi\gamma\frac{\partial u}{\partial\eta} - (x_\xi\beta + r_\xi J)\frac{\partial u}{\partial\xi} + (x_\xi J - r_\xi\beta)\frac{\partial v}{\partial\xi} + r_\xi\gamma\frac{\partial v}{\partial\eta}\right]_b = 0. \tag{15}$$

To impose the slip-boundary conditions at the free interface, equations (14) and (15) need to be first discretised at the nodes of u and v, respectively. The discretisation employs both central difference and forward difference schemes. Cartesian velocity u is determined by equation (15), and v is obtained from equation (14). Thus, the discretised forms are written as:

$$u_b = u_{b-1} + \frac{\delta\eta}{\gamma_b}\left[\left(J - \frac{r_\xi}{x_\xi}\beta\right)_b\frac{\delta v}{\delta\xi} + \left(\frac{r_\xi}{x_\xi}\gamma\right)_b\frac{\delta v}{\delta\eta} - \left(\beta + \frac{r_\xi}{x_\xi}J\right)_b\frac{\delta u}{\delta\xi}\right] \tag{16}$$

$$v_b = v_g + (u_b - u_g)\left(\frac{r_\xi}{x_\xi}\right)_b \tag{17}$$

where subscript b stands for the value at the interface, $b-1$ denotes the values on the point one grid away from the interface, and δ is a finite differential operator; the velocities u_b and v_b are the Cartesian components of fluid velocity. The central differencing scheme is employed for the first derivative terms in the ξ-direction, while a forward differencing scheme is only used for the first derivative terms in the η-direction. From equations (16) and (17) it can be seen that, if the slope of the bubble profile is large, $(\partial r/\partial x)_b = (r_\xi/x_\xi)_b = \infty$, a numerical instability is induced. To overcome this problem, the ADV method (Li and Yan, 2002b) is employed.

Employing the direct-predictor method

To obtain an increasingly improved estimate of a bubble shape, a direct predictor method (Li and Yan, 2002a) is applied using the following procedures.

(1) To predict the outline of a bubble profile (x^p, r^p), the following equations are used:

$$x_b^p = x_b^n - A_b\Delta P\frac{(r_\xi)_b}{\sqrt{\gamma_b}} \tag{18a}$$

$$r_b^p = r_b^n + A_b\Delta P\frac{(x_\xi)_b}{\sqrt{\gamma_b}} \tag{18b}$$

where the subscript b represents the values at the interface; A_b is a constant coefficient based on the maximum imbalance normal force difference, its value being specified by numerical experiments; the terms $-(r_\xi)_b/\sqrt{\gamma_b}$ and $(x_\xi)_b/\sqrt{\gamma_b}$ are the direction cosines of the normal direction of the interface profile; and the last terms are the components of the normal displacement in the x- and r-direction, respectively. The normal stress ΔP in equations (18(a),(b)) has been expressed as (Li and Yan, 2002a):

$$\Delta P = p_0 - p + \frac{2}{\gamma J \,\mathrm{Re}}\left[\gamma \frac{\partial V_\mathrm{r}}{\partial \eta} - \beta \frac{\partial V_\mathrm{r}}{\partial \xi}\right] - \frac{1}{\mathrm{We}\sqrt{\gamma}}\left(-\frac{x_\xi r_{\xi\xi} - r_\xi x_{\xi\xi}}{\gamma} + \frac{1}{r}\right). \tag{19}$$

where the three terms on the right hand side of the equation are, respectively, the pressure difference between the inside and outside of the bubble, the difference in normal viscosity stresses, and the difference in surface tension force.

(2) To get a corrected position $\left(x_b^{n+1}, r_b^{n+1}\right)$ in order to reduce the imbalance in the normal stress:

On the basis of values (x_b^p, r_b^p), final positions (x^{n+1}, r^{n+1}) can be determined as:

$$x_b^{n+1} = \mathscr{R} x_b^p \tag{20a}$$

$$r_b^{n+1} = \mathscr{R} r_b^p \tag{20b}$$

where

$$\mathscr{R} = \left(\frac{\bar{V}^{\mathrm{Old}}}{\bar{V}^{\mathrm{New}}}\right)^{\frac{1}{3}} \tag{21}$$

$$\bar{V} = \int_0^1 \pi r^2 \frac{\partial x}{\partial \xi}\,\mathrm{d}\xi \tag{22}$$

The ratio of the new volume to the old volume of bubble, $\mathscr{R}$, is used to correct the exact positions with an inner iteration at each time step.

(3) To repeat procedures (1) and (2) until the imbalance in the normal stress satisfies the pre-specified tolerance.

The application of the SCL

To deal with the flow problem with time dependent moving interface, Dermirdzic and Peric's (1990) SCL method is employed. By a first-order integration of the equation, a fully implicit time integration scheme over the control volume used for mass conservation can be expressed as

$$\frac{(J - J^0)r\Delta x\Delta r}{\Delta t} + (-u_g r_\eta + v_g x_\eta)_e r\Delta r - (-u_g r_\eta + v_g x_\eta)_w r\Delta r + (-v_g x_\xi + u_g r_\xi)_n r\Delta x - (-v_g x_\xi + u_g r_\xi)_s r\Delta x = 0 \quad (23)$$

This equation is used to update the Jacobian number to guarantee the basic requirement for space conservation.

Solution procedure

To simulate deformation of a bubble, a solution of the momentum and continuity equations is required by using an iteration procedure. Steps in such a procedure can be summarised as:

(1) assume an initial bubble shape, for example, a spherical bubble, being at rest in a stagnant liquid;

(2) generate a non-orthogonal grid to match the bubble shape;

(3) obtain convergence solutions for discretised governing equations by the SIMPLE algorithm for an estimated bubble shape;

(4) check the total normal stress. If it is not satisfied, modify the bubble profile to reduce the imbalance in the total normal stress;

(5) generate a new grid and calculate the interface velocity by step (4). Then calculate grid velocities at all nodes and update the Jacobian number by using equation (23); and

(6) repeat steps (3)-(5) untill all equations and boundary conditions are satisfied.

Validation of the code

Bubble shape

In order to validate the direct-predictor method, the shape of a bubble at $Re = 2$ and $We = 12$, $Re = 20$ and $We = 15$, $Re = 100$ and $We = 6$, and $Re = 200$ and $We = 5$ is simulated, respectively, by the steady method developed in this paper. Results and comparisons with Ryskin and Leal's (1984a-c) results are shown in Figure 3, and it can be seen that the present results are in fair agreement. On closer inspection, a very small difference in wake volume or length behind the bubble between the two sets of results may be identified; this could result from the fact that a grid of 40×40 was used in Ryskin and Leal's simulation, which may not be sufficient to get a grid independent solution.

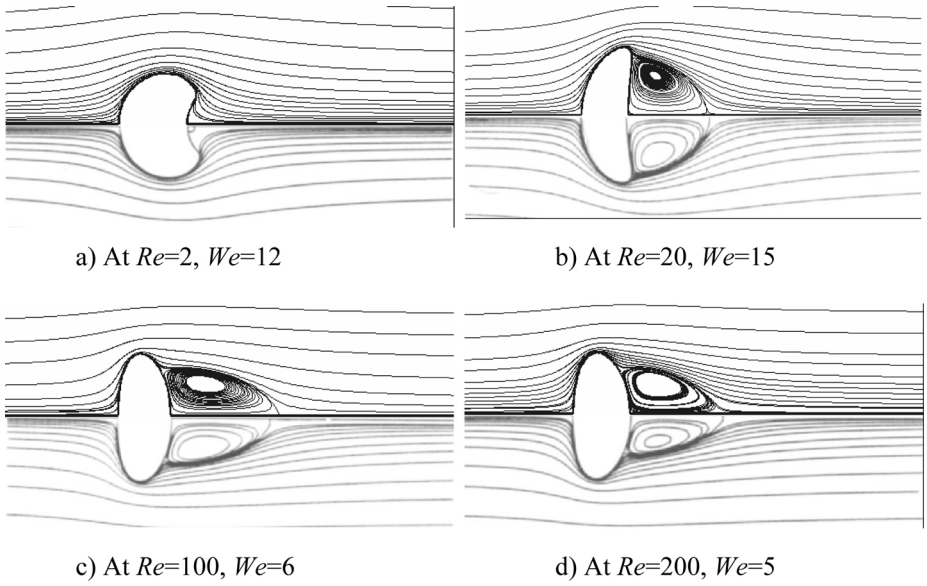

Figure 3.
Comparison of bubble shape and streamlines between present results and those of Ryskin and Leal (1984a-c)

The grid independent studies have been done by Li and Yan (2002a,b). In those work, three different grid arrangements such as 45×45, 67×67 and 91×91 were applied for the calculations and the results with grid arrangement of 67×67 was proved to be grid independent.

Rising velocity

The rising velocity of a gas bubble has been investigated experimentally for many years. Due to the complex behaviour of a rising gas bubble, in particular, a deformed bubble in a liquid, it is difficult to find a unifying analytical expression. Clift *et al.* (1978) has summarised some reasonable formulations in dealing with particle acceleration. Normally, for an unsteady motion of a particle, it is necessary to introduce the particle density explicitly because this can determine the particle inertia and the net gravity force. Thus, the rising velocity of an arbitrary gas bubble can be expressed in a general form:

$$\left(\rho_g + \frac{\rho_l}{2}\right) V_b \frac{du_T}{dt} = g(\rho_l - \rho_g)V_b - F_x - F_h, \tag{24}$$

where the subscript "g" and "l" denote gas and liquid, respectively, V_b being the volume of the gas bubble. The second term on the left-hand side of the equation is an added mass or virtual mass contribution. The first term on the right-hand side of the equation stands for a buoyancy force, the second term is the drag force in the direction of the rising bubble and the third term is called the Basset history force, which is induced by the contribution of a past acceleration. Based on the assumption made in the previous section, the gas density inside a bubble

can be ignored. The drag force is calculated by integrating all forces acting on the interface in the x-direction. According to the suggestion by Clift *et al.* (1978) and Takagi and Matsumoto (1996), the "historical" term in equation (24) is negligible. As the rising velocity of the bubble is dependent on the time-dependent drag force F_x, thus, equation (24) can be rewritten as:

$$\frac{\rho_l}{2} V_b \frac{\mathrm{d}u_T}{\mathrm{d}t} = g\rho_l V_b - F_x \tag{25}$$

This equation is normalised by the definitions of dimensionless groups of C_D, Re, Mo and Eö; and the following equations:

$$\bar{u}_T = \frac{u_T}{U_T}, \tag{26}$$

$$t = \frac{t' U_T}{d_e}, \tag{27}$$

where $\bar{u}_T$ is dimensionless velocity, t is dimensionless time, and t' is realistic time. Therefore, the dimensionless version of equation (25) is given as:

$$0.5 \frac{\mathrm{d}u_T}{\mathrm{d}t} = \frac{\mathrm{Eo}^{\frac{3}{2}}}{\mathrm{Re}^2 \mathrm{Mo}^{\frac{1}{2}}} - \frac{F_x d_e}{\rho_l V_b V_T^2} \tag{28}$$

Our predictions of rising velocity are compared in Figure 4 with the data from Mei (1994) and Takagi and Matsumoto (1996). Good agreement is apparent.

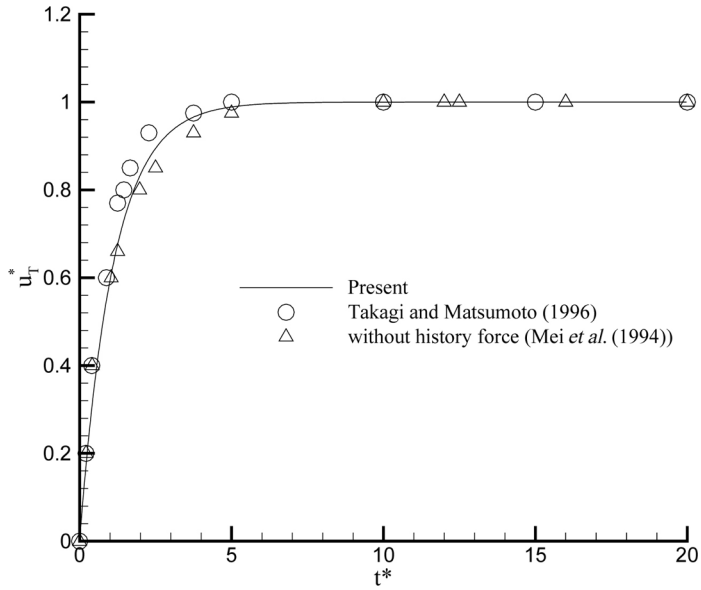

Figure 4.
Comparison of the rising velocity

Numerical results and discussion

Evolution of bubble shape

Using the numerical method and procedures presented in this paper, the unsteady deformation of a gas bubble rising in a quiescent liquid are predicted and studied. Figure 5(a)-(d) shows the results of bubble shape evolution at

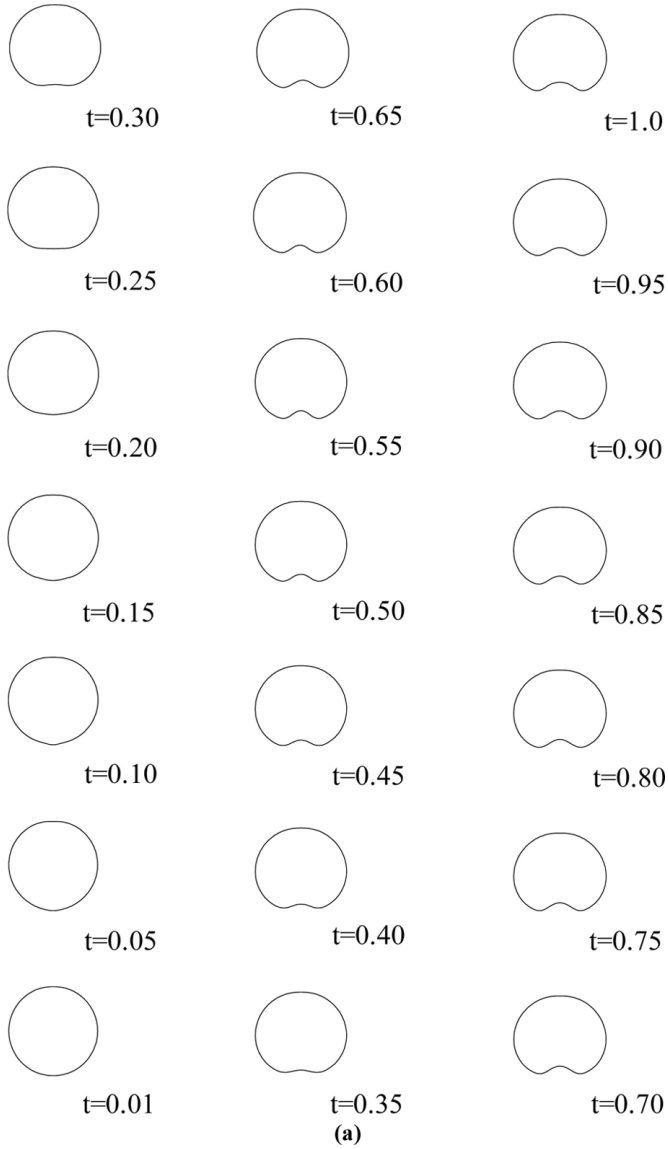

(continued)

Figure 5.
Evolution of bubble shape at (a) Re = 2 and We = 20; (b) Re = 20, We = 15; (c) Re = 50, We = 8 and (d) Re = 100, We = 6

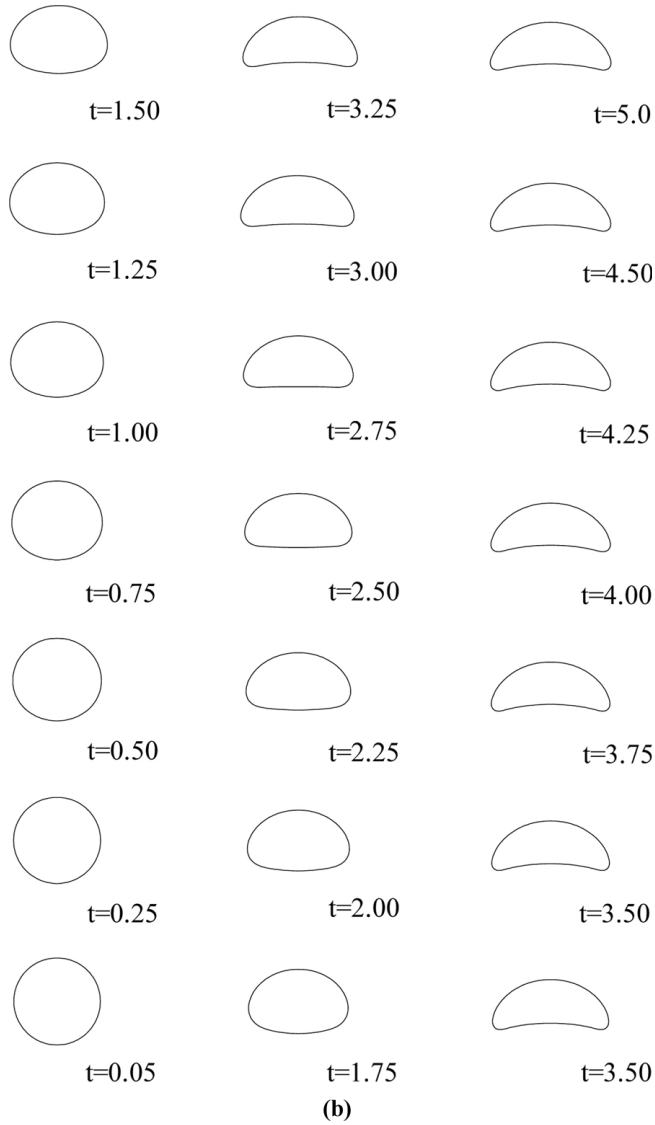

Figure 5.

(continued)

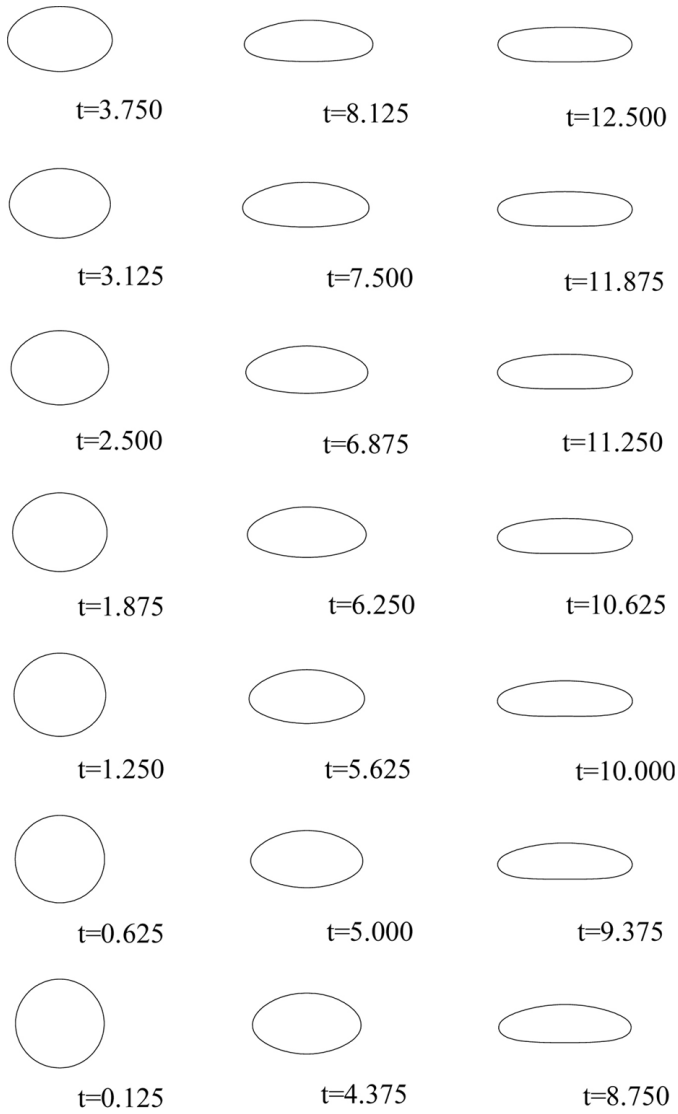

(continued)

Figure 5.

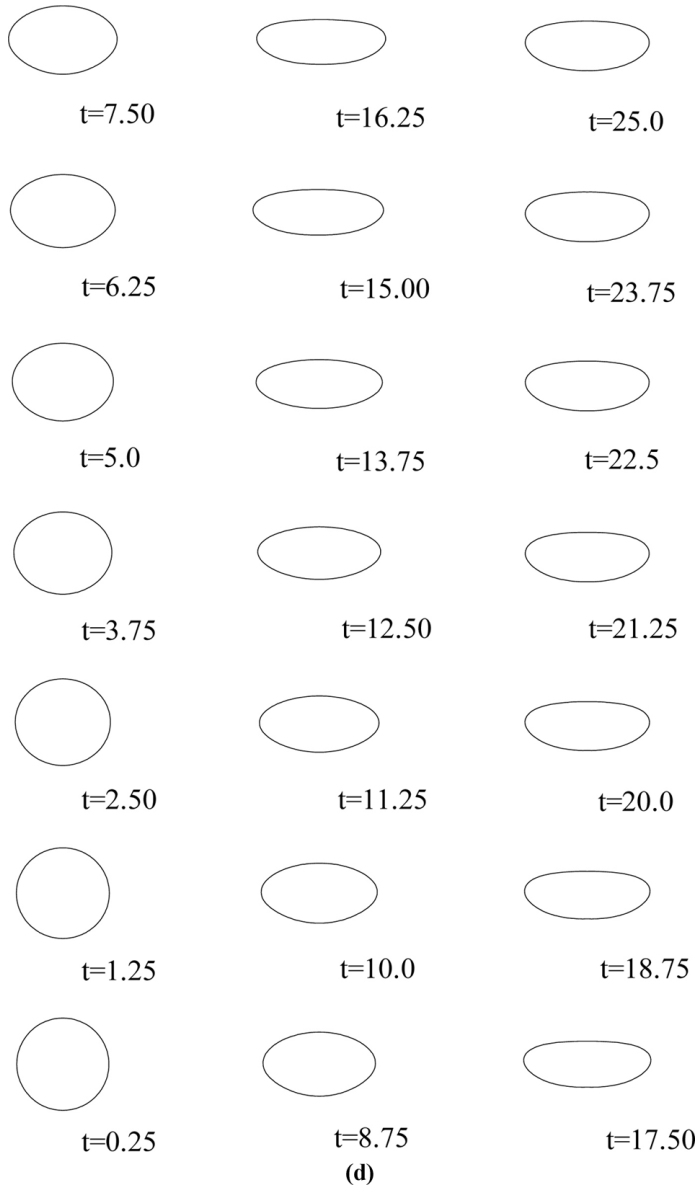

Figure 5.

different Reynolds and Weber numbers. It can be seen that the evolution of a bubble shape at the initial stages is similar in all cases and the shape deforms from spherical to oblate; however, the path of deformation occurs in different ways at the intermediate and final stages depending on the Reynolds and Weber numbers. Figure 5(a) shows the evolution of bubble shape at a low

Reynolds number and a high Weber number, such as at Re = 2 and We = 20. Figure 5(b)-(d) shows the results of bubble shape evolution with increasing Reynolds number, but decreasing Weber number. These reflect the results of interactions of inertia, viscosity and surface tension forces; the inertia force changes the bubble shape to oblate, while the surface tension force maintains the bubble as spherical. In addition, it can be seen in Figure 5(a)-(d) that the dimensionless time scales of the bubble deformation are dependent on Reynolds number. At a high Reynolds number, the time scale for a bubble reaching its terminal steady shape is longer.

It is indicated that the time scale of bubble deformation to reach its steady terminal shape is dependent on the ratio of Reynolds number to Weber number, an almost linear relationship of dimensionless time t versus the ratio of (Re/We) can be drawn as shown in Figure 6.

Propagation of concentration and temperature fields

Figures 7 and 8 show the propagation of concentration and temperature fields around a deformed bubble in water (at Schmidt number, Sc = 500 and Prandtl number, Pr = 2). It is shown that the propagation of the concentration and the temperature is mainly dependent on the evolution of the bubble deformation. At a low Reynolds number (Re = 2) and a high Weber number (We = 20), such as in Figures 7(a) and 8(a), the effect of convective heat and mass transfer on the concentration and temperature fields is weaker than that of diffusion so that the fields are uniform. At an initial deformation stage, the contours are nearly in parallel with the interfacial outline. When the bubble becomes an oblate with a flat bottom, the concentration wake and temperature wake begin to form behind the bubble. When the shape of the bubble is dimpled with a concave indentation, the volume of the wake becomes increasingly large so that an area of high concentration and temperature is formed at the rear of the bubble.

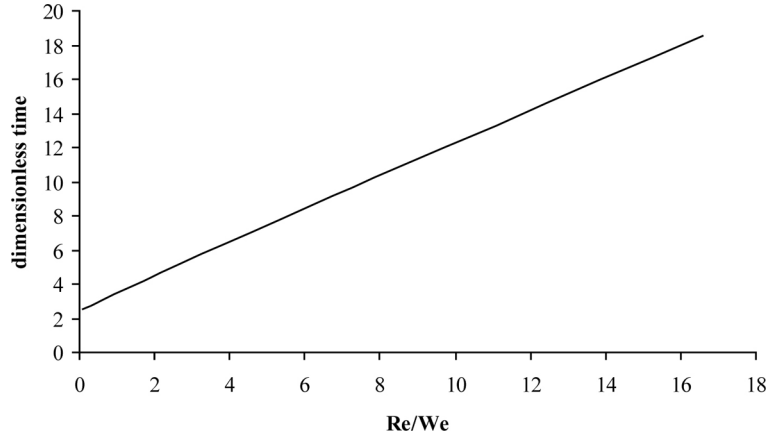

Figure 6.
Time scale for bubble's steady terminal shape versus the ratio of (Re/We)

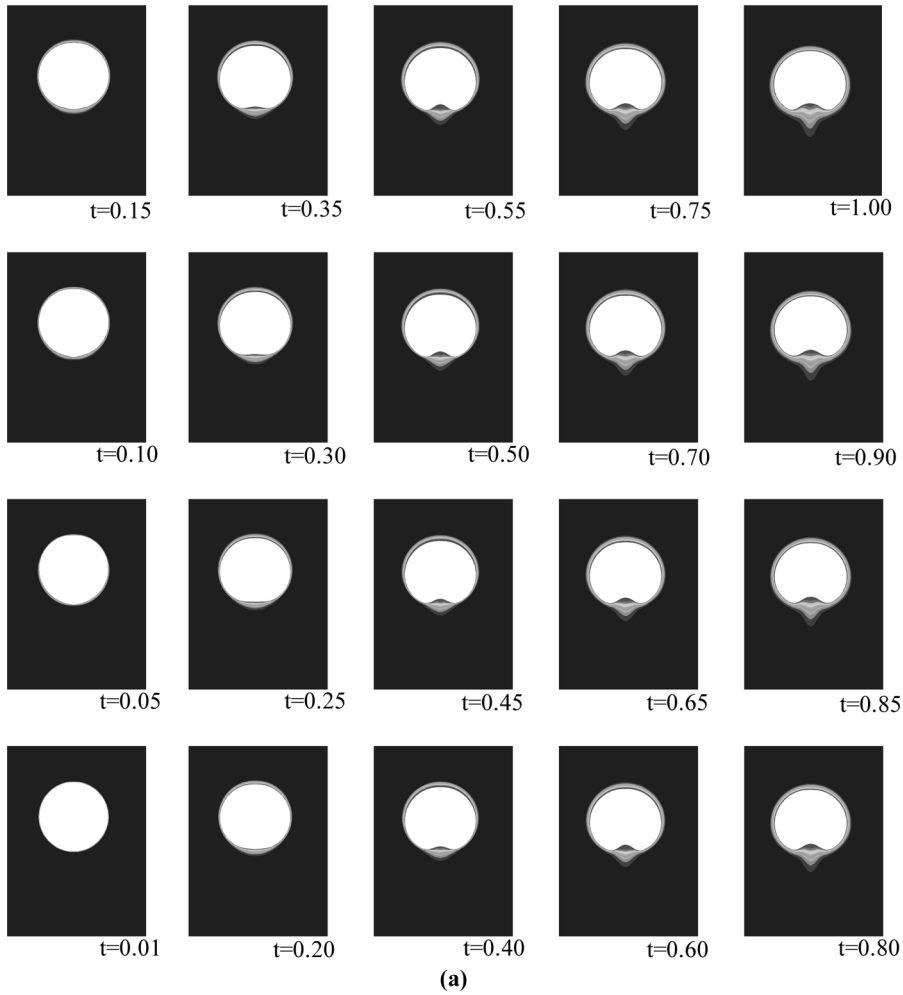

Figure 7.
Propagation of concentration field around a deformed bubble at (a) Re = 2, We = 20 and Sc = 500; (b) Re = 50, We = 8 and Sc = 500

(continued)

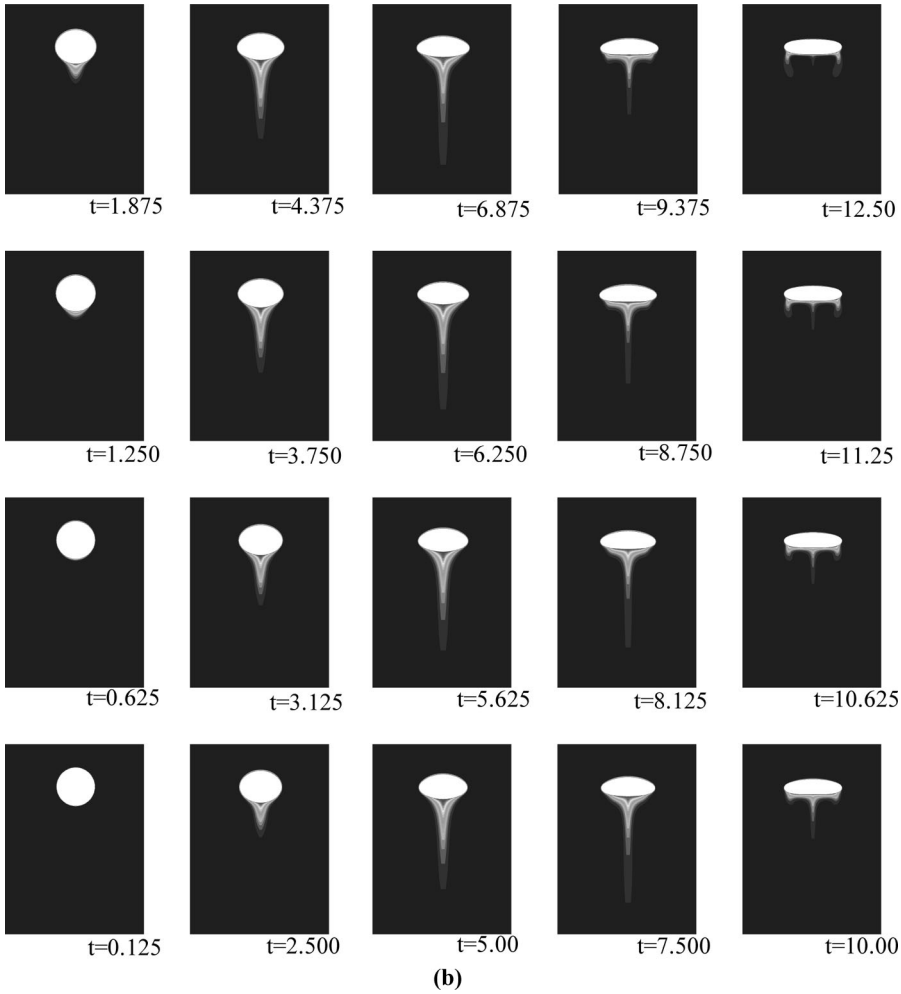
t=1.875
t=4.375
t=6.875
t=9.375
t=12.50
t=1.250
t=3.750
t=6.250
t=8.750
t=11.25
t=0.625
t=3.125
t=5.625
t=8.125
t=10.625
t=0.125
t=2.500
t=5.00
t=7.500
t=10.00
(b)

Figure 7.

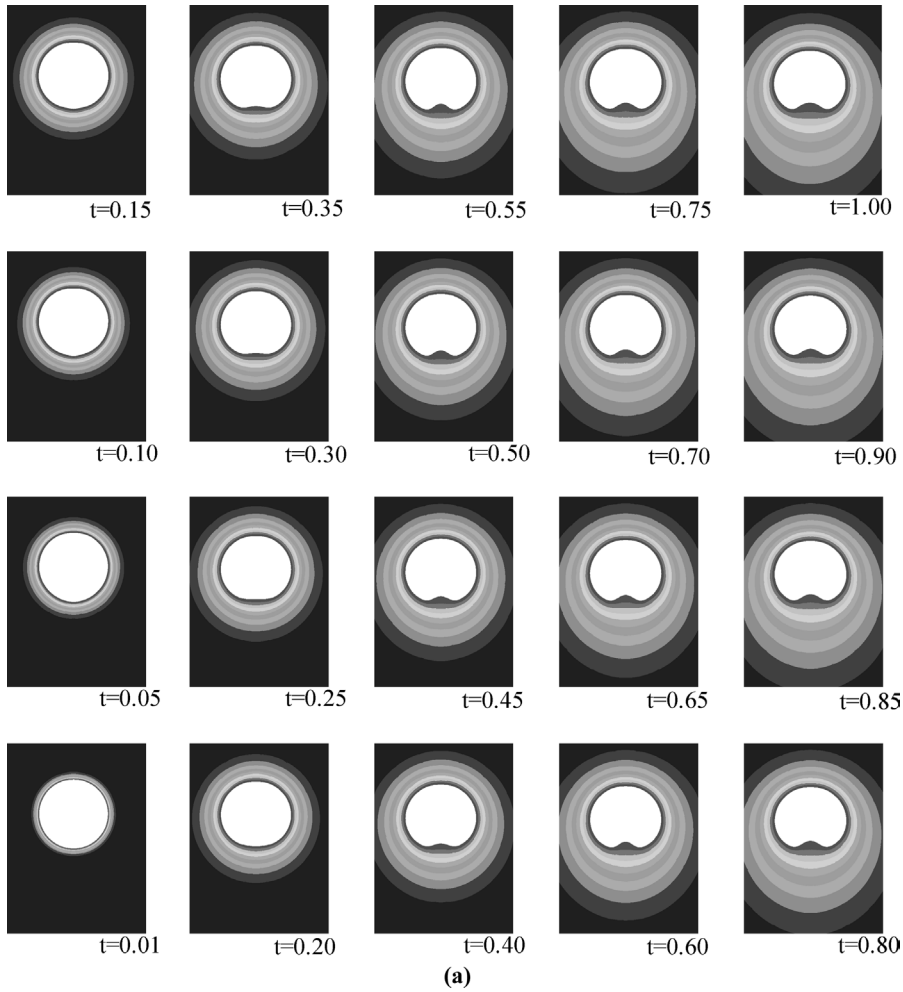

Figure 8.
Propagation of temperature field around a deformed bubble at (a) Re = 2, We = 20 and Pr = 2.0 and (b) Re = 50, We = 8 and Pr = 2

(continued)

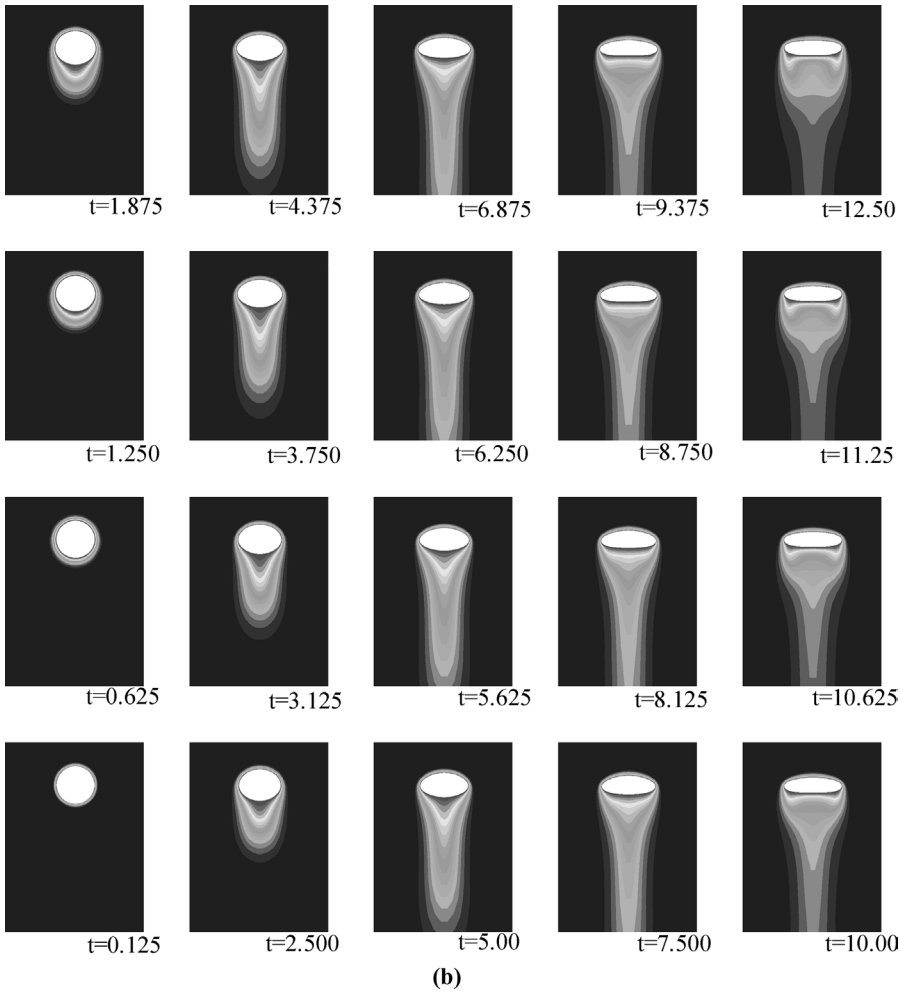

Figure 8.

With Reynolds number increasing to 50 and Weber number decreasing to 8, as shown in Figures 7(b) and 8(b), the convective transfer becomes stronger so that the volume of the wake is bigger, flow separation appears at the rear of the bubble; and this results in a striking change in the propagation of the concentration and temperature wakes.

Conclusions

In this paper, a numerical procedure is proposed for calculating the evolution of a deformed gas bubble rising in a quiescent hot liquid; on this basis, the evolution of bubble shape and the propagation of the temperature and concentration fields around the bubble are studied and simulated. For a

deformable gas bubble rising in water (at $Sc = 500$ and $Pr = 2$), the propagation of temperature and concentration fields at different Reynolds and Weber numbers is calculated and simulated. It is found that the bubble evolution at an initial stage is similar in all cases, and the path of the bubble deformation is from a spherical to an oblate; however, the deformation path is different for all cases at an intermediate stage, and in particular, at the final stages. Moreover, the time scale for a bubble to reach its steady terminal shape is dependent on the ratio of the terminal Reynolds number to the terminal Weber number, (Re/We); the t almost linearly increases with (Re/We). In addition, it is found that the bubble deformation has a significant effect on the propagation of concentration and temperature fields; and the flow separation behind a deformed bubble has a great effect on the evolution of the concentration and temperature wakes.

References

Clift, R., Grace, J.R. and Weber, M.E. (1978), *Bubbles, Drops, and Particles*, Academic Press, NY, pp. 23-8.

Dermirdzic, I. and Peric, M. (1988), "Space conservation law in finite volume calculations of fluid flow", *Int. J. Numer. Methods Fluids*, Vol. 8, pp. 1037-50.

Dermirdzic, I. and Peric, M. (1990), "Finite volume methods for prediction of fluid flow in arbitrarily shaped domains with moving boundaries", *Int. J. Numer. Methods Fluids*, Vol. 10, pp. 771-90.

Kang, I.S. and Leal, L.G. (1987), "Numerical solution of axisymmetric, unsteady free-boundary problems at finite Reynolds number, I, finite-difference scheme and its application to deformation of a bubble in a uniaxial straining flow", *Phys. Fluids*, Vol. 8, p. 1929.

Kang, I.S. and Leal, L.G. (1989), "Numerical solution of axisymmetric, unsteady free-boundary problems at finite Reynolds number, II, deformation of a bubble in a biaxial straining flow", *Phys. Fluids*, Vol. A1, p. 644.

Li, W.Z. and Yan, Y.Y. (2002a), "A predictor-correction method for solving steady terminal shape of a gas bubble rising through a quiescent liquid", *Numer. Heat Transfer*, Vol. 42 No. 1, Part B.

Li, W.Z. and Yan, Y.Y. (2002b), "An alternating dependent variables (ADV) method for treating slip-boundary conditions of free surface flows with heat and mass transfer", *Numer. Heat Transfer*, Vol. 41 No. 2, Part B, pp. 165-89.

Mei, R. (1994), "Effect of turbulence on the particle settling velocity in the nonlinear drag range", *Int. J. Multiphase Flow*, Vol. 20 No. 2, pp. 273-84.

Plesset, M.S. and Zwick, S.A. (1954), "The growth of vapor bubbles in superheated liquids", *J. Appl. Phys.*, Vol. 25 No. 4, pp. 493-500.

Ryskin, G. and Leal, L.G. (1984a), "Numerical solution of free-boundary problems in fluid mechanics. Part 1: the finite-difference technique", *J. Fluid Mech.*, Vol. 148, pp. 1-17.

Ryskin, G. and Leal, L.G. (1984b), "Numerical solution of free-boundary problems in fluid mechanics. Part 2: buoyancy-driven motion of a gas bubble through a quiescent liquid", *J. Fluid Mech.*, Vol. 148, pp. 19-35.

Ryskin, G. and Leal, L.G. (1984c), "Numerical solution of free-boundary problems in fluid mechanics. Part 3: bubble deformation in an axisymmetric straining flow", *J. Fluid Mech.*, Vol. 148, pp. 37-43.

Shyy, W., Udaykumar, H.S., Rao, M.M., and Smith, R.W. (1996), *Computational Fluid Dynamics with Moving Boundaries*, Taylor & Francis, London, pp. 21-38.

Takagi, S. and Matsumoto, Y. (1996), "Force Acting on a Rising Bubble in a Quiescent Liquid", *ASME Fluids Engineering Division Conference, 1, FED*, Vol. 236, pp. 575-80.

Takagi, S., Matsumoto, Y. and Huang, H. (1997), "Numerical analysis of a single rising bubble using boundary-fitted coordinate system", *JSME, Int. J. B*, Vol. 40 No. 1, pp. 42-50.

Thomas, P.D. and Middelcoff, J.F. (1980), "Direct control of the grid point distribution in meshes generated by elliptic equations", *AIAA, J.*, Vol. 18, pp. 625-56.

Thompson, J.F., Thames, F.C. and Mastin, C.W. (1974), "Automatic numerical generation of body-fitted curvilinear coordinate system for fields containing any number of arbitrary two dimensional bodies", *J. Comp. Phys.*, Vol. 15, p. 299.

Wittke, D.D. and Chao, B.T. (1967), "Collapse of vapour bubble with translatory motion", *J. Heat Transfer.*, Vol. 89, pp. 17-24.

Further reading

Ferziger, J.H. and Peric, M. (1999), *Computational Methods for Fluid Dynamics*, Springer, Berlin, pp. 209-33.